ELSEVIER

Physica B 292 (2000) 323–336

PHYSICA B

www.elsevier.com/locate/physb

Relaxation of spin echo signals of ^{53}Cr nuclei in Ag-doped $CdCr_2Se_4$

G.N. Abelyashev[a], V.N. Berzhansky[a], S.N. Polulyakh[a], N.A. Sergeev[b,*]

[a]*Department of Physics, Taurida National University, 95007 Simferopol, Ukraine*
[b]*Institute of Physics, University of Szczecin, ul. Wielkopolska 15, 70-451 Szczecin, Poland*

Received 15 July 1999; received in revised form 25 January 2000

Abstract

The frequency dependences of the relaxation times of NMR spin echo signals of the quadrupole nuclei ^{53}Cr were measured in the ferromagnetic semiconductor $Cd_{0.985}Ag_{0.015}Cr_2Se_4$ at the temperature $T = 4.2$ K. The experimental results were well explained by the developed theory of the two-pulse echoes relaxation. The main assumption of this theory is the assumption that the temporal fluctuations in the electron magnetization due to the fluctuations in the hyperfine and quadrupole Hamiltonians lead to the relaxation of the echo signals. It was shown that in $Cd_{0.985}Ag_{0.015}Cr_2Se_4$ there are two kinds of the quadrupole nuclei ^{53}Cr, which have quite different relaxation times. The existence of two kinds of the nuclei ^{53}Cr ($^{53}Cr(I)$ and $^{53}Cr(II)$) was connected with doping of the cadmium selenochromite with Ag^+ ions. The nuclei $^{53}Cr(II)$ are sited in the crystal ranges where the rapid electron exchange between the Cr^{4+} and Cr^{3+} ions leads to the rapid fluctuations in the local electron magnetization vector. The nuclei $^{53}Cr(I)$ are located far from these dynamical defects. The observed frequency dependence of the relaxation rate of the usual Hahn's echo signal from the nuclei $^{53}Cr(I)$ was explained by the secular theory of the echo relaxation. The nonsecular relaxation theory well explains the frequency dependence of the relaxation rate of multiquantum echo signal from the nuclei $^{53}Cr(II)$.

PACS: 76.20 + q; 76.60. – k; 76.60.Lz

Keywords: NMR in ferromagnets; Nuclear magnetic relaxation; $CdCr_2Se_4$

1. Introduction

The pulse-NMR method is one of the powerful techniques for the study of the spin dynamics in magnetically ordered materials. For the nuclear spin system with spin $I = \frac{1}{2}$, the magnetization of the electron system $\boldsymbol{M}_e$ due to the hyperfine interaction determines the NMR resonance frequencies [1,2]. On the other hand, the thermal fluctuations in the electron magnetization lead to the fluctuations in local hyperfine magnetic fields at the nuclei sites. These fluctuations in the hyperfine fields can be probed through the relaxation decays of the spin echo signals [3–9]. In the case of a spin $I = \frac{1}{2}$ system the excitation of the nuclear spin system by the two-pulse sequence causes the formation of a single echo signal observed at $t_e = \tau$ (here

* Corresponding author.
E-mail address: sergeev@uoo.univ.szczecin.pl (N.A. Sergeev).

0921-4526/00/$ - see front matter
PII: S0921-4526(00)00463-4

τ is the time interval between the RF pulses and t_e is the time interval between the end of the second pulse and the maximum of the echo signal) [1,10]. The decay of this echo signal depends on the correlation time of the fluctuating hyperfine magnetic field and may be either exponential or nonexponential [3–9].

In the case of quadrupole nuclei with $I = \frac{3}{2}$ (for example ^{53}Cr nuclei), when the quadrupole interactions of the nuclei do not equal zero, two echo signals may be observed at $t_e = \tau$ and $t_e = 3\tau$ [11–16]. The first echo signal V_τ is the usual Hahn's echo [1,10]. The NMR spectrum $V_\tau(\nu)$ recorded with the aid of this echo reflects all NMR spectral lines of the quadrupole nuclei. The frequencies of these lines depend not only on the interaction of the nuclear magnetic moment with the hyperfine magnetic field, but also on the electric quadrupole interaction of the nuclear electric quadrupole moment with the inhomogeneous electric field at the site of the nucleus [1,10]. However, the NMR spectrum $V_{3\tau}(\nu)$ recorded with the aid of the echo at $t_e = 3\tau$ consists of the NMR resonance frequencies, whose values are determined by the hyperfine interaction only [13,14]. The experimental conditions for the formation of the echo signal $V_{3\tau}$ are quite different from those for the echo V_τ [13–16]. The echo $V_{3\tau}$ appears in the case when the first RF pulse excites the three-quantum coherence in the nuclear spin system [13–15]. In order to achieve efficient excitation of the three-quantum-coherence it is necessary to selectively excite the three-quantum transition $\pm\frac{3}{2} \leftrightarrow \mp\frac{3}{2}$. The efficient excitation of this three-quantum transition depends on the carrier frequency of the RF pulses and on the relation between the amplitude of the RF pulse and the quadrupole splitting of the NMR spectrum. The optimal excitation is achieved when this relation is approximately equal to one and when the carrier frequency of the RF pulses coincides with the frequency of the $\pm\frac{1}{2} \leftrightarrow \mp\frac{1}{2}$ NMR transition [13–15]. It is necessary also that the duration of the first RF pulse exceeds the duration of the second pulse [13–15]. In magnetically ordered substances the amplitude of the RF field at the nucleus site due to the hyperfine interaction is always much greater than the external alternating RF field [1,10]. The enhancement coefficient η of the RF field depends on many factors which are not well known usually [1]. This is one of the serious limitations which does not allow to obtain experimentally the optimal echo signals $V_{3\tau}(\nu)$ (as well as the echo signals $V_\tau(\nu)$) at the different carrier frequencies of the RF pulses [13–15].

In the case of the quadrupole nuclei the thermal fluctuations in electron magnetization vector $\boldsymbol{M}_e$ lead to the fluctuation in the hyperfine interaction Hamiltonian and in the quadrupole interaction Hamiltonian too [17–20]. The existence of the two channels of the nuclear relaxation (through the hyperfine and the quadrupole interactions) is reflected in the decay of the spin echo signals of quadrupole nuclei [17–20].

In this paper we analyze the decay of two-pulse echo signals of the quadrupole nuclei ^{53}Cr in ferromagnetic semiconductor $Cd_{0.985}Ag_{0.015}Cr_2Se_4$. The paper is organized as follows: the experimental results are presented in Section 2. The experimental results contain the frequency dependences of the relaxation times of NMR spin echo signals $V_\tau(\nu)$ and $V_{3\tau}(\nu)$ of quadrupole ^{53}Cr nuclei obtained in the multidomain polycrystalline sample of $Cd_{0.985}Ag_{0.015}Cr_2Se_4$ at $T = 4.2$ K. In Section 3 we discuss the obtained experimental results using the theory of the relaxation of the two-pulse echo signals developed in the appendix. We assume that the relaxation of the spin echoes arises from the temporal fluctuations in the electron magnetization vector $\boldsymbol{M}_e$. The good agreement between the theory and experiment suggests this model of the spin echoes relaxation of the ^{53}Cr nuclei in the cadmium selenochromite doped with silver ions. From the best fit of the theory and experiment we obtained the parameters which describe the $\boldsymbol{M}_e$ fluctuations. The discussions of these parameters and the possible source of the time fluctuations in the electron magnetization vector $\boldsymbol{M}_e$ are presented in Section 4. Section 5 contains the conclusion.

2. Experimental results

The NMR measurements were made on a polycrystalline multidomain sample of $Cd_{0.985}Ag_{0.015}Cr_2Se_4$ at 4.2 K. Experiments were

performed on a home-built incoherent pulse NMR spectrometer in zero static external magnetic field. The NMR spectra of ^{53}Cr nuclei were obtained by recording the dependences of the amplitudes of the echo signals at $t_e = \tau$ and $t_e = 3\tau$ as a function of the carrier frequency ν of the RF pulses at fixed values of the amplitude and the time separation τ of the two RF pulses. The echo signals V_τ (as well as echo signals $V_{3\tau}$) were observed at equal amplitudes of the both RF pulses. For the echo V_τ the relation between the durations of the second (t_2) and the first pulses (t_1) was equal $t_2/t_1 \approx 2$. For the echo at $t_e = 3\tau$ this relation was equal $t_2/t_1 \approx 0.5$. In order to obtain the echo signals $V_{3\tau}$ it was necessary to use powerful RF pulses.

The obtained NMR spectra $V_\tau(\nu)$ and $V_{3\tau}(\nu)$ of ^{53}Cr nuclei are shown in Fig. 1. These NMR spectra coincide with NMR spectra obtained earlier [13,14,20]. In a spinel structure $CdCr_2Se_4$ the Cr nuclei are located in the octahedral lattice sites. The local symmetry of these sites is trigonal so the NMR absorption spectrum of ^{53}Cr nucleus ($I = \frac{3}{2}$) would consist of three NMR lines [1,10]. The frequencies of these lines are given by the following expressions [13,20]:

$$\nu_1 = \nu_0 + \nu_a(3\cos^2\theta_0 - 1), \quad (1)$$

$$\nu_{2,3} = \nu_0 + (\nu_a \pm \nu_Q)(3\cos^2\theta_0 - 1), \quad (2)$$

where ν_0 is the isotropic component of the NMR frequency ($\nu_0 = 44.05$ MHz [13,20]), ν_a the anisotropic part of the resonance frequency ($\nu_a = -0.55$ MHz [13,20]) and ν_Q the value of the quadrupole splitting of the NMR spectrum ($\nu_Q = 0.92$ MHz [13,20]). The angle θ_0 in Eqs. (1) and (2) is the angle between the local trigonal axis and a direction of the electron magnetization vector $\boldsymbol{M}_e$.

From Fig. 1 it follows that action of two RF pulses on $CdCr_2Se_4$ leads to simultaneous excitation of the nuclei in the domains and in the domain walls, as result of which the $V_\tau(\nu)$ and $V_{3\tau}(\nu)$ spectra are the superpositions of the spectra from the domains, which have a discrete fine structure, and of the continuum from the domain walls. The NMR spectrum of ^{53}Cr nuclei shown in Fig. 1 reflects the presence of three different types of domains in $CdCr_2Se_4$, in which the orientation of the electron

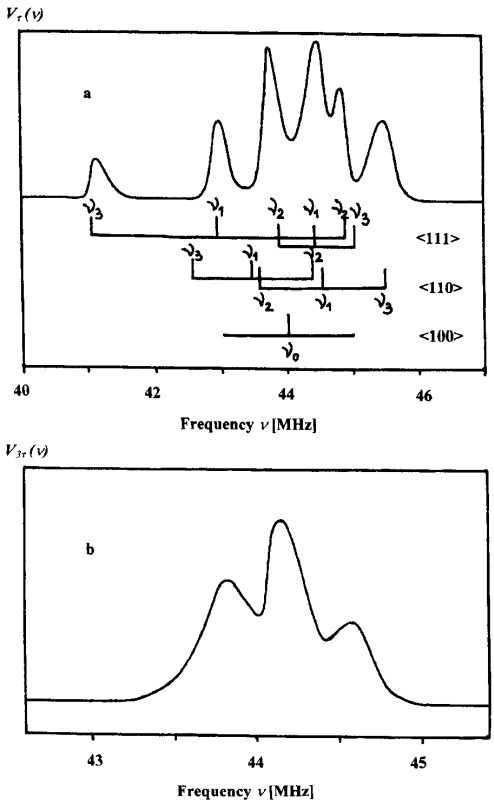

Fig. 1. The NMR spectra $V_\tau(\nu)$ (a) and $V_{3\tau}(\nu)$ (b) of ^{53}Cr nuclei in $Cd_{0.985}Ag_{0.015}Cr_2Se_4$ at $T = 4.2$ K. The vertical bars represent schematically position of NMR spectral lines ν_1, ν_2, ν_3 (Eqs. (1) and (2)) of ^{53}Cr nuclei from different type of the domains.

magnetization $\boldsymbol{M}_e$ coincides with the crystallographic directions [100], [110] and [111] [13,20,21].

It was found that the shape of the NMR spectrum $V_\tau(\nu)$ depends on the time interval τ between the exciting RF pulses. This fact suggests that the relaxation rates of the echo signals are different at different carrier frequencies of the RF pulses and that the RF pulses excite only the nuclei for which the resonance frequencies are near the excitation

frequency v. The shape of the $V_\tau(v)$ spectrum does practically not depend on the amplitude of the RF pulses.

The frequency range of the $V_{3\tau}(v)$ spectrum is much narrower than the one of the $V_\tau(v)$ spectrum and it is located in the range of the frequencies: $v_0 - v_a > v > v_0 + 2v_a$ [13,20]. The shape of the NMR spectrum $V_{3\tau}(v)$ depends not only on the time interval τ between the RF pulses but also on the amplitude of the RF pulses. This fact reflects the multiquantum nature of this echo signal. As was mentioned in the introduction the multiquantum echo signal at $t_e = 3\tau$ is very sensitive to the excitation conditions of the quadrupole nuclei ^{53}Cr by the RF pulses [13–15].

The transverse relaxation times of the echo signals were determined by observing the decay of the spin echo signals as a function of the time τ for fixed values of amplitude and carrier frequency of the exciting RF pulses. From our experiments it follows that the amplitudes of the echo signals at $t_e = \tau$ and $t_e = 3\tau$ are decreased exponentially as the pulse interval τ increases ($\tau \geqslant 10$ μs). The obtained frequency dependence of the relaxation time $T_2(\tau, v)$ of the echo signal observed at $t_e = \tau$ is shown in Fig. 2. The experimental frequency dependence of the relaxation time $T_2(3\tau, v)$ of the echo signal observed at $t_e = 3\tau$ is shown in Fig. 3.

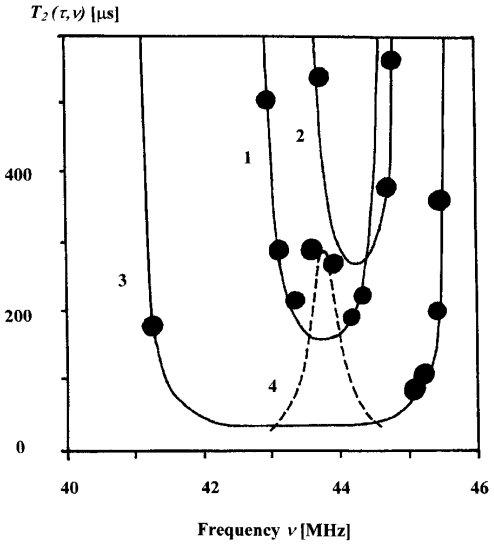

Fig. 2. Frequency dependence of the relaxation time $T_2(\tau, v)$ of ^{53}Cr nuclei in $Cd_{0.985}Ag_{0.015}Cr_2Se_4$ at $T = 4.2$ K. The solid lines are the theoretical curves obtained from the best fit of Eqs. (24)–(26), the result of our theory, to the measured values of $T_2(\tau, v)$. Curve 1 is the dependence $T_2(\tau, v_1)$; curves 2 and 3 are the dependences $T_2(\tau, v_2)$ and $T_2(\tau, v_3)$. Curve 4 (broken line) is given by Eq. (49).

3. Analysis of experimental results

In this section we shall analyze the obtained experimental results by using the developed in the appendix theory of the relaxation of the two-pulse echo signals. The main assumption of our theory is the assumption that the time fluctuations in the electron magnetization due to the fluctuations in the hyperfine and quadrupole interactions lead to the relaxation of the spin echo signals.

3.1. Hamiltonian of quadrupole nucleus in magnetic solids

The Hamiltonian of a quadrupole nucleus in magnetic solids contains the hyperfine interaction Hamiltonian and the quadrupole interaction Hamiltonian and can be written as [1,10]

$$H = H_{HF} + H_Q, \tag{3}$$

The hyperfine interaction Hamiltonian in the case of axial symmetry of the hyperfine magnetic tensor has the form ($\hbar = 1$)[10]

$$H_{HF} = -\omega_i I_z - \omega_a(3\cos^2\theta - 1)I_z - \tfrac{3}{2}\omega_a \sin(2\theta)I_x. \tag{4}$$

The frequency ω_i is determined in magnetically ordered substances by the isotropic hyperfine magnetic field (HF) at the site of the nucleus; ω_a is determined by the anisotropic HF field at the nuclear site. The angle θ in Eq. (4) is the angle between the principal axis of the HF interaction tensor and electron magnetization direction $\boldsymbol{M}_e$.

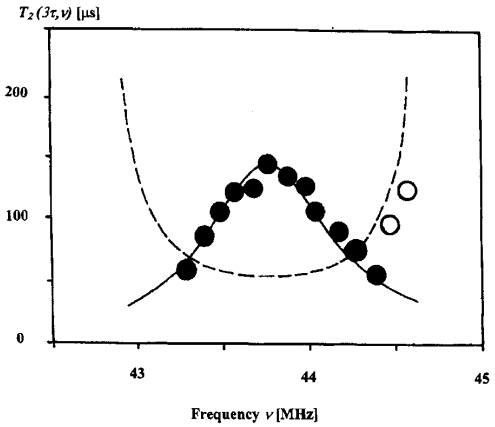

Fig. 3. Frequency dependence of the relaxation time $T_2(3\tau, \nu_1)$ of ^{53}Cr nuclei in $Cd_{0.985}Ag_{0.015}Cr_2Se_4$ at $T = 4.2$ K. The solid line is the theoretical curve obtained from the best fit of Eq. (38), the result of our theory, to the measured values of $T_2(3\tau, \nu_1)$ (black circles). The broken line is the curve $\frac{1}{3}T_2(\tau, \nu_1)$ with parameters defined from curve 1 in Fig. 2.

Assuming the symmetry of the electric field gradient (EFG) tensor at the site of the nucleus is axial too and the principal axis of the EFG tensor coincides with the principal axis of the HF tensor we may write the quadrupole interaction Hamiltonian in the form ($\hbar = 1$) [10]

$$H_Q = \frac{\omega_Q}{2}(3\cos^2\theta - 1)\left[I_z^2 - \frac{I(I+1)}{3}\right] + \frac{\omega_Q}{2}\sin(2\theta)(I_zI_x + I_xI_z) + \frac{\omega_Q}{4}\sin^2\theta(I_+^2 + I_-^2), \quad (5)$$

where $\omega_Q = 3e^2qQ/4I(2I-1)$ is the quadrupole interaction constant of the nucleus [10].

In the Hamiltonians H_{HF} and H_Q the z-axis is the quantization axis for the nuclear spin and in magnetically ordered materials this axis coincides with the direction of the electron magnetization $\boldsymbol{M}_e$ [1,10].

Now we assume that the temporal fluctuation of the interaction Hamiltonian (3) arises from the thermal fluctuations of the electron magnetization vector $\boldsymbol{M}_e$ [17–20]. Neglecting the fluctuation in ω_a we may write the interaction Hamiltonian $H(t)$ as a sum of static and time-dependent parts [17–19]

$$H(t) = H_0 + H_1(t). \quad (6)$$

The static part of $H(t)$ has the form

$$H_0 = -\omega_0 I_z - \omega_a(3\cos^2\theta_0 - 1)I_z + \frac{\omega_Q}{2}(3\cos^2\theta_0 - 1)\left[I_z^2 - \frac{I(I+1)}{3}\right], \quad (7)$$

where $\omega_0 = \overline{\omega_i(t)}$ and $\theta_0 = \overline{\theta(t)}$ are the time-average values of $\omega_i(t)$ and $\theta(t)$.

The time-dependent part in the Hamiltonian $H(t)$ contains two terms

$$H_1(t) = H_{1s}(t) + H_{1ns}(t). \quad (8)$$

Here $H_{1s}(t)$ is the secular part of $H_1(t)$

$$H_{1s}(t) = -\delta\omega_i(t)I_z + \left\{3\omega_a I_z - \frac{3\omega_Q}{2} \times \left[I_z^2 - \frac{I(I+1)}{3}\right]\right\}\sin(2\theta_0)\,\delta\theta(t). \quad (9)$$

In Eq. (9) $\delta\omega_i(t) = \omega_i(t) - \omega_0$ describes the fluctuation in the isotropic part of the hyperfine magnetic field and $\delta\theta(t) = \theta(t) - \theta_0$ describes the fluctuation in the direction of the electron magnetization vector $\boldsymbol{M}_e$.

The nonsecular part of the Hamiltonian $H_1(t)$ has the form [19]

$$H_{1ns}(t) = \left[-3\omega_a\cos(2\theta_0)I_x + \omega_Q\cos(2\theta_0) \times (I_zI_x + I_xI_z) + \frac{\omega_Q}{4}\sin(2\theta_0)(I_+^2 + I_-^2)\right]\delta\theta(t). \quad (10)$$

In Eq. (7) we omitted the static nonsecular terms of the interaction Hamiltonian because in magnetically ordered substances the term $(-\omega_0 I_Z)$ in the Hamiltonian H_0 is the largest term [1,2].

We shall assume that the fluctuations of ω_i and θ are Gaussian stochastic processes and the

correlation functions of these values are of exponential type

$$\overline{\delta\omega_i(t')\delta\omega_i(t'-\tau)} = \sigma_\omega^2 e^{-|\tau|/\tau_{c\omega}}, \tag{11}$$

$$\overline{\delta\theta(t')\delta\theta(t'-\tau)} = \sigma_\theta^2 e^{-|\tau|/\tau_{c\omega}}. \tag{12}$$

In Eq. (11) $\tau_{c\omega}$ is the correlation time of the fluctuating frequency $\omega_i(t)$; $\sigma_\omega^2 = \overline{\delta\omega_i^2(t)} - \omega_0^2$ is the mean-square fluctuation of the random variable $\omega_i(t)$. In Eq. (12) $\tau_{c\theta}$ is the correlation time of the time fluctuating angle $\theta(t)$; $\sigma_\theta^2 = \overline{\delta\theta^2(t)} - \theta_0^2$ is the mean-square fluctuation of the random variable $\theta(t)$.

In Sections 3.2 and 3.3 we shall analyze the relaxation of the two-pulse echoes of quadrupole nuclei with spin $I = \frac{3}{2}$. We shall assume that the RF pulses excite only those nuclei which have resonance frequencies at the carrier frequency of the exciting RF pulses.

3.2. Secular relaxation of spin echo signals

In this subsection we consider the relaxation of the two-pulse echoes of quadrupole nuclei with spin $I = \frac{3}{2}$ taking into account only the secular term $H_{1s}(t)$ in the fluctuating Hamiltonian (8). As was mentioned in the introduction, for a quadrupole nucleus with spin $I = \frac{3}{2}$ the two echo signal at $t_e = \tau$ and $t_e = 3\tau$ can be formed [12–16]. At first we consider the relaxation of the echo signal $V_\tau(v)$.

3.2.1. Relaxation of $V_\tau(v)$ echo signal

If the carrier frequency of the RF pulses coincides with the frequency defined by Eq. (1) and so the RF pulses selectively excite only the NMR transitions $\pm\frac{1}{2} \leftrightarrow \mp\frac{1}{2}$, the quantum values a, b, c, d in Eq. (A.28) are [13,17–19]

$$a = c = -\tfrac{1}{2}, \quad b = d = \tfrac{1}{2}. \tag{13}$$

Using these quantum numbers we obtain from Eqs. (A.28)–(A.32) the following expression for the amplitude $V_\tau(v_1)$ of the two pulse echo signal observed at $t_e = \tau$:

$$V_\tau(v_1) = V_\tau(0, v_1)\exp\left[-\frac{2\tau}{T_{2s}(\tau, v_1)}\right], \tag{14}$$

where

$$V_\tau(0, v_1) = \langle -\tfrac{1}{2}|R_2|\tfrac{1}{2}\rangle\langle\tfrac{1}{2}|R_1 I_z R_1^{-1}|-\tfrac{1}{2}\rangle \times \langle -\tfrac{1}{2}|R_2^{-1}|\tfrac{1}{2}\rangle\langle\tfrac{1}{2}|I_+|-\tfrac{1}{2}\rangle \tag{15}$$

is the amplitude of the echo signal at $\tau \to 0$ and

$$T_{2s}^{-1}(\tau, v_1) = -2J_{-1/2,-1/2,1/2,1/2}(0) + J_{1/2,1/2,1/2,1/2}(0) + J_{-1/2,-1/2,-1/2,-1/2}(0). \tag{16}$$

is the relaxation rate of the echo signal $V_\tau(v_1)$. The subscript (s) in T_{2s}^{-1} denotes that the source of the echo signal relaxation is the secular fluctuating terms of the hyperfine and quadrupole Hamiltonians.

Inserting the secular Hamiltonian $H_{1s}(t)$ in Eq. (A.18) and using the correlation functions (11) and (12) we have from Eqs. (A.30)–(A.32)

$$T_{2s}^{-1}(\tau, v_1) = \sigma_\omega^2\tau_{c\omega} + 9\omega_a^2\sigma_\theta^2\tau_{c\theta}\sin^2(2\theta_0). \tag{17}$$

If the carrier frequency v_{RF} of the RF pulses coincides with the frequency v_2 or v_3 defined by Eq. (2) and so the RF pulses selectively excite only the NMR transitions $\pm\frac{3}{2} \leftrightarrow \pm\frac{1}{2}$, the quantum values a, b, c, d in Eq. (A.28) are [13,17–19]

$$v_{RF} = v_2, \quad a = c = \tfrac{1}{2}, \quad b = d = \tfrac{3}{2}, \tag{18}$$

$$v_{RF} = v_3, \quad a = c = -\tfrac{3}{2}, \quad b = d = -\tfrac{1}{2}. \tag{19}$$

Using these quantum numbers we obtain from Eqs. (A.30)–(A.32) the following expression for the relaxation rates of the echo signals $V_\tau(v_2)$ and $V_\tau(v_3)$:

$$T_{2s}^{-1}(\tau, v_{2,3}) = \sigma_\omega^2\tau_{c\omega} + 9(\omega_a \pm \omega_Q)^2\sigma_\theta^2\tau_{c\theta}\sin^2(2\theta_0). \tag{20}$$

From Eqs. (17) and (20) it follows that the relaxation rates of the echo signals $V_\tau(v_i)$ $(i = 1, 2, 3)$ have the same angular dependences and may be written as

$$T_{2s}^{-1}(\tau, v_i) = A + B_i\sin^2(2\theta_0), \tag{21}$$

where

$$A = \sigma_\omega^2\tau_{c\omega} \tag{22}$$

and

$$B_1 = 9\omega_a^2\sigma_\theta^2\tau_{c\theta},$$

$$B_{2,3} = 9(\omega_a \pm \omega_Q)^2\sigma_\theta^2\tau_{c\theta}. \quad (23)$$

Using Eqs. (1) and (2) and the above-mentioned values ν_0, ν_a and ν_Q, it is possible to replace in Eq. (21) the variable θ_0 by the frequency ν_i

$$42.95\ \text{MHz} \leqslant \nu_1 \leqslant 44.6\ \text{MHz}$$

$$T_{2s}^{-1}(\tau,\nu_1) = A + \frac{4}{9}B_1\left(2 - \frac{\nu_1-\nu_0}{\nu_a}\right) \times\left(1 + \frac{\nu_1-\nu_0}{\nu_a}\right), \quad (24)$$

$$43.68\ \text{MHz} \leqslant \nu_2 \leqslant 44.79\ \text{MHz}$$

$$T_{2s}^{-1}(\tau,\nu_2) = A + \frac{4}{9}B_2\left(2 - \frac{\nu_2-\nu_0}{\nu_a+\nu_Q}\right) \times\left(1 + \frac{\nu_2-\nu_0}{\nu_a+\nu_Q}\right), \quad (25)$$

$$41.11\ \text{MHz} \leqslant \nu_3 \leqslant 45.52\ \text{MHz}$$

$$T_{2s}^{-1}(\tau,\nu_3) = A + \frac{4}{9}B_3\left(2 - \frac{\nu_3-\nu_0}{\nu_a-\nu_Q}\right) \times\left(1 + \frac{\nu_3-\nu_0}{\nu_a-\nu_Q}\right). \quad (26)$$

The solid lines shown in Fig. 2 represent the theoretical frequency dependences obtained from the best fit of Eqs. (24)–(26) to the observed values of $T_2(\tau,\nu)$. As it is seen, the theoretical curves agree well with the experimental results. The fitting parameters are

$$\sigma_\omega^2\tau_{c\omega} = (1.65 \pm 0.02)\times 10^3\,\frac{\text{rad}^2}{\text{s}}, \quad (27)$$

$$\sigma_\theta^2\tau_{c\theta} = (4.5 \pm 0.3)\times 10^{-11}\ \text{s}. \quad (28)$$

From Fig. 2 we see that there is a discrepancy between the experimental and theoretical $T_2(\tau,\nu_1)$ values at $\nu_1 \approx \nu_0 + (\nu_a/2)$ or at $\theta_0 \approx \pi/4$. We shall consider the possible source of this discrepancy in Section 4.

3.2.2. Secular relaxation of multiquantum $V_{3\tau}(\nu_1)$ echo signal

Now, we consider the relaxation of the echo signal at $t_e = 3\tau$ retaining in the fluctuating Hamiltonian (8) only the secular term $H_{1s}(t)$ too. Multiquantum echo signal $V_{3\tau}$ observed only when the carrier frequency ν_{RF} of the RF pulses coincides with the frequency ν_1 [13–15]. For this echo signal the quantum values a,b,c,d are [13,17–19]

$$a = -\tfrac{1}{2},\quad b = \tfrac{3}{2},\quad c = -\tfrac{3}{2},\quad d = \tfrac{1}{2}. \quad (29)$$

Using these quantum numbers we have from Eqs. (A.28)–(A.32) the following expression for the amplitude of the echo signal $V_{3\tau}(\nu_1)$

$$V_{3\tau}(\nu_1) = V_{3\tau}(0,\nu_1)\exp\left[-\frac{4\tau}{T_{2s}(3\tau,\nu_1)}\right], \quad (30)$$

where

$$V_{3\tau}(0,\nu_1) = \langle -\tfrac{1}{2}|R_2|\tfrac{3}{2}\rangle\langle\tfrac{3}{2}|R_1 I_Z R_1^{-1}|-\tfrac{3}{2}\rangle \times\langle -\tfrac{3}{2}|R_2^{-1}|\tfrac{1}{2}\rangle\langle\tfrac{1}{2}|I_+|-\tfrac{1}{2}\rangle \quad (31)$$

is the echo signal amplitude at $\tau \to 0$ and

$$\begin{aligned} T_{2s}^{-1}(3\tau,\nu_1) = {} & -\tfrac{1}{2}J_{3/2,3/2,-3/2,-3/2}(0) \\ & -\tfrac{3}{2}J_{-1/2,-1/2,1/2,1/2}(0) \\ & +\tfrac{1}{4}[J_{3/2,3/2,3/2,3/2}(0) \\ & +J_{-3/2,-3/2,-3/2,-3/2}(0)] \\ & +\tfrac{3}{4}[J_{-1/2,-1/2,-1/2,-1/2}(0) \\ & +J_{1/2,1/2,1/2,1/2}(0)] \end{aligned} \quad (32)$$

is the relaxation rate of the echo signal at $t_e = 3\tau$.

Inserting the secular Hamiltonian $H_{1s}(t)$ in Eq. (A.18) and using the correlation functions (11) and (12) we obtain from Eqs. (A.31) and (A.32)

$$T_{2s}^{-1}(3\tau,\nu_1) = 3T_{2s}^{-1}(\tau,\nu_1) = 3A + 3B_1\sin^2(2\theta_0). \quad (33)$$

The broken line in Fig. 3 represents the theoretical frequency dependence of $T_{2s}(3\tau,\nu_1)$ defined by Eq. (33). As it is seen only two experimental points (the open circles) coincide with this frequency dependence. Eq. (33) does not explain the characteristic frequency dependence of $T_{2s}(3\tau,\nu_1)$, that is, the value of $T_{2s}(3\tau,\nu_1)$ takes a maximum value at

$\nu_1 \approx \nu_0 + (\nu_a/2)$ or at $\theta_0 \approx \pi/4$. In order to understand the source of this discrepancy we shall consider in Section 3.3 the relaxation of the multiquantum echo signal $V_{3\tau}(\nu_1)$ retaining in the fluctuating Hamiltonian (8) the nonsecular terms too.

3.3. Nonsecular relaxation of multiquantum $V_{3\tau}(\nu_1)$ echo signal

Using the full Hamiltonian (8) we obtain the following expression for the amplitude of the echo signal $V_{3\tau}(\nu_1)$:

$$V_{3\tau}(\nu_1) = V_{3\tau}(0,\nu_1)\exp\left[-\frac{4\tau}{T_2(3\tau,\nu_1)}\right], \tag{34}$$

where $V_{3\tau}(0,\nu_1)$ is defined by Eq. (31) and

$$T_2^{-1}(3\tau,\nu_1) = T_{2s}^{-1}(3\tau,\nu_1) + T_{2ns}^{-1}(3\tau,\nu_1). \tag{35}$$

Here $T_{2s}^{-1}(3\tau,\nu_1)$ is the secular relaxation rate defined by Eq. (33) and

$$\begin{aligned} T_{2ns}^{-1}(3\tau,\nu_1) = {} & 9\omega_a^2\sigma_\theta^2\tau_{c\theta}\cos^2(2\theta_0)\left[\frac{3}{21+(2\pi\nu_1\tau_{c\theta})^2}\right. \\ & + \frac{1}{12}(3-2\xi)^2\frac{1}{1+(2\pi\nu_3\tau_{c\theta})^2} \\ & \left. + \frac{1}{12}(3+2\xi)^2\frac{1}{1+(2\pi\nu_2\tau_{c\theta})^2}\right] \\ & + \frac{3}{16}\omega_Q^2\sigma_\theta^2\tau_{c\theta}\sin^2(2\theta_0) \\ & \times\left\{\frac{1}{1+[2\pi(\nu_1+\nu_2)\tau_{c\theta}]^2}\right. \\ & \left. + \frac{1}{1+[2\pi(\nu_1+\nu_3)\tau_{c\theta}]^2}\right\} \end{aligned} \tag{36}$$

is the nonsecular relaxation rate of the echo $V_{3\tau}(\nu_1)$. Here $\xi = \omega_Q/\omega_a$.

We proceed to discuss only the important special case of the so-called extreme narrowing limit ($2\pi\nu\tau_{c\theta} \ll 1$) for which all spectral density $J_{abcd}(\omega)$ converge to $J_{abcd}(0)$ [10]. It is expected that the nonsecular relaxation can yield a significant contribution to the full relaxation rates of the quadrupole echoes only in this limiting case [10].

For the case of extreme narrowing limit we have from Eq. (36)

$$\begin{aligned} T_{2ns}^{-1}(3\tau,\nu_1) = {} & 27\omega_a^2\sigma_\theta^2\tau_{c\theta}\cos^2(2\theta_0) \\ & + \tfrac{3}{8}\omega_Q^2\sigma_\theta^2\tau_{c\theta}[1+15\cos^2(2\theta_0)]. \end{aligned} \tag{37}$$

Combining Eqs. (37) with (33) we obtain the following expression for the full relaxation rate of the spin echo $V_{3\tau}(\nu_1)$:

$$T_2^{-1}(3\tau,\nu_1) = C + D\cos^2(2\theta_0), \tag{38}$$

where

$$C = 3\sigma_\omega^2\tau_{c\omega} + \left[24\left(\frac{\omega_a}{\omega_Q}\right)^2 + \frac{1}{3}\right]\frac{D}{5} \tag{39}$$

and

$$D = \tfrac{45}{8}\omega_Q^2\sigma_\theta^2\tau_{c\theta}. \tag{40}$$

The solid line in Fig. 3 represents the theoretical frequency dependence of $T_2(3\tau,\nu_1)$ defined by Eq. (38). As it is seen the frequency dependence (38) well describes the observed dependence of $T_2(3\tau,\nu_1)$. The obtained fitting parameters are

$$C = (6.7 \pm 0.2)\times 10^3\,\frac{\text{rad}^2}{\text{s}}, \tag{41}$$

$$D = (23.3 \pm 0.9)\times 10^3\,\frac{\text{rad}^2}{\text{s}}. \tag{42}$$

4. Discussion

The obtained results suggest that in $Cd_{0.985}Ag_{0.015}Cr_2Se_4$ there are two kinds of the ^{53}Cr nuclei, which have quite different relaxation times. The nuclei of the first kind $^{53}Cr(I)$ give the main contribution to the echo signal $V_\tau(\nu)$. In the echo signal $V_{3\tau}(\nu)$ these nuclei are observed only at $\nu > 44.5$ MHz (the open circles in Fig. 3). The nuclei of the second kind $^{53}Cr(II)$ give the main contribution to the echo $V_{3\tau}(\nu_1)$ (the black circles in Fig. 3).

As shown in the analysis in Section 3.2.1, the relaxation of the spin echo signals of the $^{53}Cr(I)$ nuclei was well explained by the secular theory of the spin echo relaxation. The secular approximation is applicable when $2\pi\nu_i\tau_{c\theta} \gg 1$ [10]. The value

of $\tau_{c\theta}$ could not be obtained from our experiments. However, we may estimate this value assuming that $\nu_i \approx 44$ MHz and $2\pi\nu_i\tau_{c\theta} > 10$. Then we obtain

$$\tau_{c\theta}(^{53}\mathrm{Cr(I)}) > 4\times10^{-8}\ \mathrm{s}. \tag{43}$$

Assuming that $\tau_{c\omega} \approx \tau_{c\theta}$ we have from Eqs. (27) and (28)

$$\frac{\sigma_\omega(^{53}\mathrm{Cr(I)})}{2\pi} < 32\ \mathrm{kHz} \tag{44}$$

and

$$\sigma_\theta(^{53}\mathrm{Cr(I)}) < 2^0. \tag{45}$$

The relaxation of the spin echo signal $V_{3\tau}(\nu)$ of the ^{53}Cr(II) nuclei was well explained by the nonsecular theory of the spin echo relaxation. In the extreme narrowing limit we have $2\pi\nu_i\tau_{c\theta} \ll 1$. If we assume again $\nu_i \approx 44$ MHz, then from condition $2\pi\nu_i\tau_{c\theta} < 0.1$ we obtain

$$\tau_{c\theta}(^{53}\mathrm{Cr(II)}) < 4\times10^{-10}\ \mathrm{s}. \tag{46}$$

Using Eqs. (41) and (42) and assuming that $C > [24(\omega_a/\omega_Q)^2 + \frac{1}{3}]D/5$ the following condition is easily obtained

$$\left|\frac{\omega_a(^{53}\mathrm{Cr(II)})}{\omega_Q(^{53}\mathrm{Cr(II)})}\right| < 0.2. \tag{47}$$

From comparison of Eqs. (46) and (43) it follows that the frequency $(\tau_{c\theta}^{-1})$ of the fluctuation in the direction of the electron magnetization $\boldsymbol{M}_e$ for the nuclei ^{53}Cr(II) exceeds the one for the nuclei ^{53}Cr(I).

The echo signal $V_{3\tau}(\nu_1)$ is observed in the same frequency range as the echo signal $V_\tau(\nu_1)$. This experimental fact indicates that the value of ω_a for the nuclei ^{53}Cr(II) is of the same order as the one for the nuclei ^{53}Cr(I). Then, from the condition (47) it follows that the electric field gradient (ω_Q) at the sites of the nuclei ^{53}Cr(II) exceeds the one for the nuclei ^{53}Cr(I) (for the nuclei ^{53}Cr(I) we have $|\omega_a(^{53}\mathrm{Cr(I)})/\omega_Q(^{53}\mathrm{Cr(I)})| = 0.6$).

In order to estimate the contribution of the nuclei ^{53}Cr(II) to the echo signal $V_\tau(\nu)$ we considered the nonsecular relaxation of the echo signal $V_\tau(\nu_1)$. The following expression for the nonsecular relaxation rate of this echo for the case of the extreme narrowing limit has been obtained:

$$T_2^{-1}(\tau,\nu_1) = \sigma_\omega^2\tau_{c\omega} + [9\omega_a^2 + \tfrac{3}{8}\omega_Q^2]\sigma_\theta^2\tau_{c\theta} + \tfrac{45}{2}(\omega_a^2 + \tfrac{1}{4}\omega_Q^2)\sigma_\theta^2\tau_{c\theta}\cos^2(2\theta_0). \tag{48}$$

Using Eqs. (39) and (40) we have from Eq. (48)

$$T_2^{-1}(\tau,\nu_1) = \tfrac{1}{3}C + \tfrac{2}{45}D + \left[1 + 4\left(\frac{\omega_a}{\omega_Q}\right)^2\right]D\cos^2(2\theta_0), \tag{49}$$

where C and D are determined by Eqs. (39) and (40).

The broken line in Fig. 2 represents the theoretical curve (49) with parameters C and D defined by Eqs. (41) and (42) ($|\omega_a/\omega_Q| = 0.2$). As is seen, the relaxation time of the echo signal $V_\tau(\nu_1)$ from the nuclei ^{53}Cr(II) is not smaller than the one from nuclei ^{53}Cr(I) at $\nu_1 \approx \nu_0 + (\nu_a/2)$. So, in this frequency region the nuclei ^{53}Cr(II) give also the contribution to the echo signal $V_\tau(\nu_1)$. This fact explains why there is the discrepancy between the experimental and theoretical $T_2(\tau,\nu_1)$ values at $\nu_1 \approx \nu_0 + (\nu_a/2)$.

It is reasonable to assume that the existence of two kinds of ^{53}Cr nuclei in $Cd_{0.985}Ag_{0.015}Cr_2Se_4$ is connected with the doping of $CdCr_2Se_4$ with Ag^+ ions. The doping of the cadmium selenochromite with silver ions produces, as a result of electric charge compensation, Cr^{4+} impurities. It is obvious that the electric charge defects Ag^+ and Cr^{4+} induce distortions of the crystal lattice and lead to the increase of the electric field gradients (ω_Q) of the nuclei ^{53}Cr sited near the defects. So, the ^{53}Cr nuclei are divided into two kinds of nuclei: the nuclei ^{53}Cr(I) are the nuclei located far from the defects and the nuclei ^{53}Cr(II) are the nuclei sited near defects.

The different relaxation times of the nuclei ^{53}Cr(I) and ^{53}Cr(II) are probably connected with the dynamical nature of the Cr^{4+} defects [20]. We assume that electron exchange between the Cr^{4+} and Cr^{3+} ions located inside the defect region leads to rapid fluctuations in the local electron magnetization. So, the nuclei ^{53}Cr(II) located in these defect

regions "feel" the rapidly fluctuating electron magnetization, due to the hyperfine and quadrupole interactions. The rate of this fluctuations highly exceeds the one for the nuclei ^{53}Cr(I) which are far from defects.

5. Conclusion

We measured the relaxation times of the two-pulse spin echo signals of the ^{53}Cr nuclei in the ferromagnetic semiconductor $Cd_{0.985}Ag_{0.015}Cr_2Se_4$ at the temperature $T = 4.2$ K. The relaxation rates $T_2^{-1}(\tau, \nu_i)$ and $T_2^{-1}(3\tau, \nu_1)$ of the echo signals at $t_e = \tau$ and $t_e = 3\tau$ exhibit characteristic frequency (angular) dependences. The dependence of the relaxation rate $T_2^{-1}(\tau, \nu_i)$ on the angle θ_0 between the local trigonal symmetry axis and a direction of the electron magnetization vector $\boldsymbol{M}_e$ has the form: $T_2^{-1}(\tau, \nu_i) = A + B_i \sin^2(2\theta_0)$. The angular dependence of the relaxation rate $T_2^{-1}(3\tau, \nu_1)$ has the form: $T_2^{-1}(3\tau, \nu_1) = C + D\cos^2(2\theta_0)$.

In order to explain the experimental results we developed the theory of the relaxation of the two-pulse echo signals. The main assumption of this theory is the assumption that the temporal fluctuations in the electron magnetization vector $\boldsymbol{M}_e$ lead to the fluctuations in the hyperfine and quadrupole interaction Hamiltonians. From analysis of the experimental results follows that the secular approximation of the developed theory well explains the observed frequency dependence of $T_2^{-1}(\tau, \nu_i)$. The experimental frequency dependence of $T_2^{-1}(3\tau, \nu_1)$, however, could not be explained by the secular theory of the spin echo relaxation. We calculated the relaxation rate $T_2^{-1}(3\tau, \nu_1)$ including the nonsecular term of the fluctuating hyperfine and quadrupole Hamiltonians. It was found that nonsecular theory of the spin echo relaxation well explains the experimental frequency dependence of the relaxation rate $T_2^{-1}(3\tau, \nu_1)$.

The existence of two different channels ("secular" and "nonsecular") for the relaxation of the echo signals $V_\tau(\nu)$ and $V_{3\tau}(\nu)$ suggest that in $Cd_{0.985}Ag_{0.015}Cr_2Se_4$ there are two kinds of the ^{53}Cr nuclei. The quite different relaxation times of these nuclei (^{53}Cr(I) and ^{53}Cr(II)) we explained assuming that the nuclei ^{53}Cr(II) are located in the defect regions which contain the ions Cr^{4+} and Ag^{+}. The nuclei ^{53}Cr(I) located far from the defect regions. In the defect regions the fast electron exchange between the Cr^{4+} and Cr^{3+} ions induces rapid fluctuations in the local electron magnetization. These rapid fluctuations in $\boldsymbol{M}_e$ lead to rapid fluctuations in the hyperfine and quadrupole Hamiltonians of the nuclei ^{53}Cr(II) located in the defect regions. The correlation times $\tau_{c\omega}$ and $\tau_{c\theta}$ of these fluctuations are very small in comparison with the inverse values of the NMR frequencies ($2\pi\nu_i\tau_{c\omega} \ll 1$; $2\pi\nu_i\tau_{c\theta} \ll 1$). This fact explains why the nonsecular relaxation theory well describes the experimental frequency dependence $T_2^{-1}(3\tau, \nu_1)$. The calculated nonsecular relaxation time of the nuclei ^{53}Cr(II) $T_2(\tau, \nu_1)$ is not small in comparison with one for the the nuclei ^{53}Cr(I) in the frequency region $\nu_1 \approx \nu_0 + (\nu_a/2)$. So, the nuclei ^{53}Cr(II) could be observed by the spin echo $V_\tau(\nu_1)$ at $\nu_1 \approx \nu_0 + (\nu_a/2)$.

The nuclei Cr(I) are located far from the dynamical defects $Cr^{4+} \leftrightarrow Cr^{3+}$ and so the influence of the electron exchange between the Cr^{4+} and Cr^{3+} ions on the fluctuations in the hyperfine and quadrupole Hamiltonians of these nuclei is small ($2\pi\nu_i\tau_{c\omega} \gg 1$; $2\pi\nu_i\tau_{c\theta} \gg 1$). This fact explains why the experimental frequency dependence $T_2^{-1}(\tau, \nu)$ of the nuclei ^{53}Cr(I) was well explained by the secular theory of the spin echo relaxation. From the calculated frequency dependence of the relaxation time $T_2(3\tau, \nu_1)$ for the nuclei ^{53}Cr(I) it follows that this time is small than the one of the nuclei ^{53}Cr(II) practically in the whole frequency region. So, the nuclei ^{53}Cr(II) give the main contribution to the echo signal observed at $t_e = 3\tau$.

In conclusion, we point out that the investigations of the relaxation of the spin echo signal $V_\tau(\nu)$ in $Cd_{1-x}Ag_xCr_2Se_4$ with various contents of the Ag ions demonstrate that the rate $T_2^{-1}(\tau, \nu_i)$ of spin echo decay increases with increasing Ag content [20]. This fact indicates that the increase in the impurity concentration should enhance the amplitudes (σ_ω^2, σ_θ^2) and the rates ($\tau_{c\omega}^{-1}$, $\tau_{c\theta}^{-1}$) in the fluctuations of the local electron magnetization in the region where nuclei ^{53}Cr(I) sit.

In order to have a better understanding of the physical mechanism of the temporal fluctuation in the electron magnetization $\boldsymbol{M}_e$ further experiments

under different conditions (temperature, external static magnetic field, various contents of Ag^+ ions) are necessary.

Acknowledgements

This work was supported, in part, by the International Soros Science Education Program through Grant NAPU072083. N.A.S. is grateful to Szczecin University for financial support (Grants No. 503-224002-370 and No. 504-234002-957). The authors are indebted to Dr. Yu.V. Fedotov for valuable contributions and technical assistance. We wish to express our gratitude to the referee for his valuable comments.

Appendix. Relaxation of two-pulse echo signals

The Hamiltonian ($\hbar = 1$) of a spin system we shall consider consists in general of two terms

$$H(t) = H_0 + H_1(t). \tag{A.1}$$

The first part H_0 of the Hamiltonian is obtained by averaging $H(t)$ over the time

$$H_0 = \overline{H(t)} = \lim_{(t\to\infty)} \frac{1}{t}\int_0^t H(t')\,dt', \tag{A.2}$$

and the second part $H_1(t)$ is the fluctuating part

$$H_1(t) = H(t) - \overline{H(t)}. \tag{A.3}$$

Let us consider a response of a spin system to a two-pulses sequence $R_1 - \tau - R_2 - t$, where R_1 and R_2 describe the actions of the first and second RF pulses. We shall assume that during the action of RF pulses the fluctuating part $H_1(t)$ of the Hamiltonian may be omitted. We choose also as our starting point the following well-known equation for the reduced spin density matrix $\rho^*(t)$ [10,22–24]

$$\rho^*(t) = \rho^*(0) - \int_0^t dt' \times \int_0^\infty [[\rho^*(0), H_1^*(t')], H_1^*(t'-t'')]\,dt''. \tag{A.4}$$

The approximations inherent in Eq. (A.4) are thoroughly discussed by Abragam [10]. Eq. (4) is valid if the changes in the density matrix are small on the time scale τ_c characteristic for the random fluctuations of the Hamiltonian $H_1(t)$ ($\|\overline{H_1^2(t)}\|\tau_c^2 \ll 1$) and $\tau_c \ll t$.

In Eq. (A.4)

$$\rho^*(t) = e^{iH_0t}\rho(t)e^{-iH_0t} \tag{A.5}$$

and

$$H_1^*(t) = e^{iH_0t}H_1(t)e^{-iH_0t}. \tag{A.6}$$

The general expression for the signal $V(\tau, t)$ following after a two-pulse sequence is given by [10]

$$V(\tau, t) \sim \mathrm{Tr}\{\overline{\rho(\tau, t)}I_+\}, \tag{A.7}$$

where $\overline{\rho(\tau, t)}$ is the spin density matrix averaged over the random fluctuations of the Hamiltonian $H_1(t)$.

Using Eq. (A.4) it is easy to obtain the following expression for the averaged spin density matrix $\overline{\rho(\tau, t)}$:

$$\overline{\rho(\tau, t)} = A_0(\tau, t) - A_1(\tau, t) - A_2(\tau, t). \tag{A.8}$$

Here

$$A_0(\tau, t) = e^{-iH_0t}R_2e^{-iH_0\tau}\rho(0)e^{iH_0\tau}R_2^{-1}e^{iH_0t}, \tag{A.9}$$

$$A_1(\tau, t) = e^{-iH_0t}R_2e^{-iH_0\tau}\left\{\int_0^\tau dt' \times \int_0^\infty \overline{[[\rho(0), H_1^*(t')], H_1^*(t'-t'')]}\,dt''\right\} \times e^{iH_0\tau}R_2^{-1}e^{iH_0t}, \tag{A.10}$$

$$A_2(\tau, t) = e^{-iH_0t}\left\{\int_0^t dt' \int_0^\infty \overline{[[R_2e^{-iH_0\tau}\rho(0)e^{iH_0\tau}R_2^{-1}, H_1^*(t')], H_1^*(t'-t'')]}\,dt''\right\} \times e^{iH_0t} \tag{A.11}$$

and

$$\rho(0) = R_1I_zR_1^{-1} \tag{A.12}$$

is spin density matrix after the first RF pulse.

The first term in Eq. (A.8) describes the response of the spin system to the two-pulses sequence in the

case when the fluctuations of Hamiltonian (A.1) do not exist ($H_1(t) = 0$). Exclusively this term in the average spin density matrix determines the conditions at which the echo signal may be formed. Substituting only the term $A_0(\tau, t)$ into Eq. (A.7) yields

$$\mathrm{Tr}\{A_0(\tau,t)I_+\} = \sum_{a,b,c,d} \langle a|R_2|b\rangle\langle b|\rho(0)|c\rangle \times \langle c|R_2^{-1}|d\rangle\langle d|I_+|a\rangle \times e^{i[(E_a - E_d)t - (E_b - E_c)\tau]}, \quad (A.13)$$

where E_a and $|a\rangle$ are the eigenvalues and eigenfunctions of the Hamiltonian H_0

$$H_0|a\rangle = E_a|a\rangle. \quad (A.14)$$

From Eq. (A.13) it follows that an echo signal will be observed at the time $t = t_e$ when t_e is equal

$$t_e = \tau\frac{E_b - E_c}{E_d - E_a}. \quad (A.15)$$

Consider now the term $A_1(\tau, t)$ in Eq. (A.8). Using Eq. (A.14) the matrix element $\langle a|A_1(\tau,t)|d\rangle$ can be written as

$$\langle a|A_1(\tau,t)|d\rangle = \sum_{b,c} \langle a|R_2|b\rangle\langle b|\overline{K(\tau)}|c\rangle\langle c|R_2^{-1}|d\rangle \times \exp\{i[(E_d - E_a)t - (E_b - E_c)\tau]\}, \quad (A.16)$$

where

$$\langle b|\overline{K(\tau)}|c\rangle = \sum_{e,f} \langle b|\rho(0)|e\rangle \int_0^\tau e^{i(E_c - E_e)t'}\,dt' \times \int_0^\infty G_{efcf}(t', t'')e^{i(E_e - E_f)t''}\,dt'' - \sum_{e,f} \langle e|\rho(0)|f\rangle \int_0^\tau e^{i(E_b + E_f - E_c - E_e)t'}\,dt' \times \int_0^\infty G_{befc}(t', t'')e^{i(E_e - E_f)t''}\,dt''$$

$$- \sum_{e,f} \langle e|\rho(0)|f\rangle \int_0^\tau e^{i(E_b + E_f - E_c - E_e)t'}\,dt' \times \int_0^\infty G_{fcbe}(t', t'')e^{i(E_e - E_b)t''}\,dt'' + \sum_{e,f} \langle f|\rho(0)|c\rangle \int_0^\tau e^{i(E_b - E_f)t'} \times \int_0^\infty G_{efbe}(t', t'')e^{i(E_e - E_b)t''}\,dt'' \quad (A.17)$$

and

$$G_{abcd}(t', t'') = \overline{\langle a|H_1(t')|b\rangle\langle c|H_1(t' - t'')|d\rangle} \quad (A.18)$$

are the correlation functions of the random Hamiltonian $H_1(t)$.

If the random process leading to the fluctuations of $H_1(t)$ is stationary the correlation functions $G_{abcd}(t', t'')$ depend only on t'' [10]. Introducing the frequencies ω_{ab}

$$\omega_{ab} = E_a - E_b \quad (A.19)$$

and defining the spectral density functions as [10]

$$J_{abcd}(\omega) = \int_0^\infty G_{abcd}(t'')e^{i\omega t''}\,dt'', \quad (A.20)$$

we obtain

$$\langle b|\overline{K(\tau)}|c\rangle = \sum_{e,f} \left\{ \langle b|\rho(0)|e\rangle J_{efcf}(\omega_{cf}) \int_0^\tau e^{i\omega_{cf}t'}\,dt' - \langle e|\rho(0)|f\rangle[J_{befc}(\omega_{cf}) + J_{fcbe}(\omega_{eb})] \times \int_0^\tau e^{i(\omega_{bc} - \omega_{cf})t'}\,dt' + \langle f|\rho(0)|c\rangle J_{efbe}(\omega_{eb}) \int_0^\tau e^{i\omega_{bf}t'}\,dt' \right\}. \quad (A.21)$$

In Eq. (A.21) the terms $\int_0^\tau \exp(i\omega t')\,dt'$ with $\omega \neq 0$ are unimportant, because these terms oscillate with high frequencies and on the time scale $(0,\tau)$ give

zero [10]. Retaining in Eq. (A.21) only the terms for which $\omega = 0$ gives

$$\langle b|\overline{K(\tau)}|c\rangle = \tau\{ -\langle b|\rho(0)|c\rangle[2J_{bbcc}(0) + \sum_f [J_{cffc}(\omega_{cf}) + J_{fbbf}(\omega_{fb})] \times [\langle b|\rho(0)|c\rangle - \delta_{bc}\langle f|\rho(0)|f\rangle]\}. \quad (A.22)$$

Inserting Eq. (A.22) into Eq. (A.16) we obtain

$$\langle a|A_1(\tau,t)|d\rangle = \tau\Big\{\sum_{b,c}\langle a|R_2|b\rangle\langle b|\rho(0)|c\rangle\langle c|R_2^{-1}|d\rangle \times e^{i[(E_d-E_a)t-(E_b-E_c)\tau]}\Big[-2J_{bbcc}(0) + \sum_f [J_{cffc}(\omega_{cf}) + J_{fbbf}(\omega_{fb})]\Big] - e^{i(E_d-E_a)t}\sum_{b,c}\langle a|R_2|b\rangle\langle c|\rho(0)|c\rangle \times \langle b|R_2^{-1}|d\rangle[J_{bccb}(\omega_{bc}) + J_{cbbc}(\omega_{cb})]\Big\}. \quad (A.23)$$

Here we used the following properties of the spectral density functions [10]:

$$J_{abcd}(\omega) = J_{cdab}(\omega). \quad (A.24)$$

Eq. (A.23) contains two types of the high-frequency oscillate terms: $\exp[i(\omega_{da}t - \omega_{bc}\tau)]$ and $\exp(i\omega_{da}t)$. For the time $t = t_e$ the first exponential according to Eq. (A.15) equals unity for all times τ. The second exponential terms depend on t only and may be omitted at the echo signals consideration [10]. Omitting these oscillating terms we may write Eq. (A.23) in the form

$$\langle a|A_1(\tau,t)|d\rangle = \tau\Big\{\sum_{b,c}\langle a|R_2|b\rangle\langle b|\rho(0)|c\rangle\langle c|R_2^{-1}|d\rangle \times\Big[-2J_{bbcc}(0) + \sum_f [J_{cffc}(\omega_{cf}) + J_{fbbf}(\omega_{fb})]\Big]\Big\}. \quad (A.25)$$

The same consideration for the term $A_2(\tau,t)$ in Eq. (A.8) gives the following expression for the matrix element $\langle a|A_2(\tau,t)|d\rangle$:

$$\langle a|A_2(\tau,t)|d\rangle = t_e\Big\{\sum_{b,c}\langle a|R_2|b\rangle\langle b|\rho(0)|c\rangle\langle|R_2^{-1}|d\rangle \times\Big[-2J_{aadd}(0) + \sum_f [J_{dffd}(\omega_{cf}) + J_{faaf}(\omega_{fa})]\Big]\Big\}. \quad (A.26)$$

Inserting Eqs. (A.9), (A.25) and (A.26) into Eq. (A.8) yields for the matrix element $\langle a|\overline{\rho(\tau,t)}|d\rangle$

$$\langle a|\overline{\rho(\tau,t)}|d\rangle = \sum_{b,c}\langle a|R_2|b\rangle\langle b|\rho(0)|c\rangle\langle c|R_2^{-1}|d\rangle \times\Big\{1 - \tau\Big[-2J_{bbcc}(0) + \sum_f [J_{cffc}(\omega_{cf}) + J_{fbbf}(\omega_{fb})]\Big] - t_e\Big[-2J_{aadd}(0) + \sum_f [J_{dffd}(\omega_{df}) + J_{faaf}(\omega_{fa})]\Big]\Big\}. \quad (A.27)$$

Using Eq. (A.27) we obtain from Eq. (A.7) the following general expression for the two-pulse echo signal:

$$V(\tau,t_e) = \sum_{a,b,c,d} A_{abcd}R_{abcd}(\tau,t_e). \quad (A.28)$$

The matrix elements A_{abcd} in Eq. (A.28) are independent of the time fluctuaions of the interaction Hamiltonian $H_1(t)$ and have the form

$$A_{abcd} = \langle a|R_2|b\rangle\langle b|R_1 I_z R_1^{-1}|c\rangle \langle c|R_2^{-1}|d\rangle\langle d|I_+|a\rangle. \quad (A.29)$$

The relaxation of echo signals is described by the matrix elements $R_{abcd}(\tau,t)$

$$R_{abcd}(\tau,t) = 1 - \tau T_{2bc}^{-1} - t_e T_{2ad}^{-1} \approx \exp(-\tau T_{2bc}^{-1} - t_e T_{2ad}^{-1}), \quad (A.30)$$

where

$$T_{2bc}^{-1} = -2J_{bbcc}(0) + \sum_f [J_{bffb}(\omega_{fb}) + J_{cffc}(\omega_{cf})] \tag{A.31}$$

and

$$T_{2ad}^{-1} = -2J_{aadd}(0) + \sum_f [J_{affa}(\omega_{fa}) + J_{dffd}(\omega_{df})]. \tag{A.32}$$

References

[1] E.A. Turov, M.P. Petrov, Nuclear Magnetic Resonance in Ferromagnets, Halstead-Wiley, New York, 1972.
[2] C.H. Cobb, V. Jaccarino, M.A. Buttler, J.P. Remeika, H. Yasuoka, Phys. Rev. B 7 (1973) 307.
[3] S.K. Ghosh, Phys. Rev. B 5 (1972) 174.
[4] T. Kohmoto, T. Goto, S. Maegawa, N. Fujiwara, Y. Fukuda, M. Kunitomo, M. Mekata, Phys. Rev. B 49 (1994) 6028.
[5] M.P. Petrov, A.P. Paugurt, Sov. Phys. Solid State 12 (1970) 2284.
[6] V.N. Berzhansky, S.N. Polulyakh, Sov. Phys. Solid State 31 (1989) 1423.
[7] G.N. Abelyashev, S.N. Polulyakh, V.N. Berzhansky, N.A. Sergeev, J. Magn. Magn. Mater. 147 (1995) 305.
[8] G.N. Abelyashev, S.N. Polulyakh, V.N. Berzhansky, N.A. Sergeev, JETP 81 (1995) 1132.
[9] V.N. Berzhansky, A.I. Gorbovanov, S.N. Polulyakh, N.V. Pronina, Phys. Solid State 40 (1998) 1494.
[10] A. Abragam, Principles of Nuclear Magnetism, Clarendon Press, Oxford, 1961.
[11] I. Solomon, Phys. Rev. 110 (1958) 61.
[12] H. Abe, H. Yasuoka, A. Hirai, J. Phys. Soc. Japan 21 (1966) 77.
[13] G.N. Abelyashev, V.N. Berzhansky, N.A. Sergeev, Yu.V. Fedotov, JETP 67 (1988) 127.
[14] G.N. Abelyashev, V.N. Berzhansky, N.A. Sergeev, Yu.V. Fedotov, Phys. Lett. A 133 (1988) 263.
[15] G.N. Abelyashev, V.N. Berzhansky, S.N. Polulyakh, N.A. Sergeev, Yu.V. Fedotov, Sov. Phys. JETP 100 (1991) 1981.
[16] P.P. Man, Phys. Rev. B 52 (1995) 9418.
[17] S.N. Polulyakh, N.A. Sergeev, JETP 81 (1995) 7.
[18] N.A. Sergeev, S.N. Polulyakh, Acta Phys. 8 (1997) 7 (University of Szczecin, Poland).
[19] S.N. Polulyakh, N.A. Sergeev, Acta Phys. 10 (1999) University of Szczecin, Poland, in press.
[20] G.N. Abelyashev, V.N. Berzhansky, Yu.V. Fedotov, S.N. Polulyakh, N.A. Sergeev, J. Magn. Magn. Mater. 184 (1998) 222.
[21] G.N. Abelyashev, V.N. Berzhansky, Yu.V. Fedotov, Pisma JETF 45 (1987) 34.
[22] R.K. Wangsness, F. Bloch, Phys. Rev. 89 (1953) 728.
[23] F. Bloch, Phys. Rev. 102 (1956) 104.
[24] A.G. Redfield, IBM J. 1 (1957) 19.